Li *et al.*
Chinese Journal of Mechanical Engineering (2024) 37:165
https://doi.org/10.1186/s10033-024-01142-1

Chinese Journal of Mechanical Engineering

ORIGINAL ARTICLE

Open Access

Study on the Relationship Between Vibration Signals in CFRP Grinding and Grinding Mechanism

Lichen Li[1], Fangyuan Wang[1], Pengda Song[1], Kai Jin[1*], Lei Chu[1*], Sansan Ding[2], Guido A. Berti[3] and Luca Quagliato[4]

Abstract

In the process of grinding carbon fiber reinforced polymer (CFRP), the changing state of acceleration vibration signal is closely related to the grinding surface quality. Therefore, the time domain and frequency domain signal changes in acceleration can be used to monitor and control the grinding process to improve machining quality and efficiency. In this paper, changes in acceleration frequency domain signals under different grinding angles are studied, and the relationship between the vibration forms of acceleration frequency domain signals at the beginning, middle and end of grinding as well as the surface morphology and quality of the corresponding grinding position is studied. Combined with the micro-morphology of the grinding area, it can be seen that, a high frequency and low amplitude vibration can improve the grinding surface quality, but a high amplitude will have a negative impact on the grinding quality. The acceleration vibration during grinding is more stable and the corresponding surface quality is better. With an increase in grinding angle, the maximum amplitude of acceleration first increases and then decreases. The length of the surface fiber also initially decreases and then increases. Lastly, the resin residue first increases and then decreases. The purpose of this study is to provide a theoretical basis for the subsequent grinding state adjustment.

Keywords CFRP, Grinding mechanism, Acceleration signal, Roughness

1 Introduction

Carbon fiber reinforced polymer (CFRP), as an excellent lightweight material, is widely used in the fields of aerospace and rail transit due to its high specific strength and stiffness, excellent corrosion resistance, and excellent fatigue resistance. Due to the pursuit of lightweight and high strength in transportation, CFRP can be used as key structural components, such as aircraft skin and car casings [1–3]. To meet the application requirements, CFRP is typically machined via various processing methods, including cutting, milling, and grinding. Ultrasonic waves [4, 5] can effectively assist in drilling, milling, and grinding processes, improving the surface quality of the processed materials compared to traditional methods [6]. Li et al. [7] found that ultrasonic waves can effectively reduce cutting forces and improve surface quality. Balaji et al. [8] not only compared and summarized the rotational ultrasonic processing of CFRP with dry grinding and wet grinding, but also elucidated the processing mechanism of CFRP from the angles of fiber orientation and tribology, providing guidance for future CFRP processing using rotational ultrasonic techniques. Gao et al.

*Correspondence:
Kai Jin
jinkai@ouc.edu.cn
Lei Chu
chulei@ouc.edu.cn
[1] College of Material Science and Technology, Ocean University of China, Qingdao 266404, China
[2] CRRC Qingdao Sifang Locomotive & Rolling Stock Co., Ltd., Qingdao 266111, China
[3] Department of Management and Engineering, University of Padua, 36100 Vicenza, Italy
[4] Division of Mechanical and Biomedical Engineering, Ewha Womans University, Seoul 03760, Republic of Korea

Springer Open

© The Author(s) 2024. **Open Access** This article is licensed under a Creative Commons Attribution 4.0 International License, which permits use, sharing, adaptation, distribution and reproduction in any medium or format, as long as you give appropriate credit to the original author(s) and the source, provide a link to the Creative Commons licence, and indicate if changes were made. The images or other third party material in this article are included in the article's Creative Commons licence, unless indicated otherwise in a credit line to the material. If material is not included in the article's Creative Commons licence and your intended use is not permitted by statutory regulation or exceeds the permitted use, you will need to obtain permission directly from the copyright holder. To view a copy of this licence, visit http://creativecommons.org/licenses/by/4.0/.

[9] studied the relationship between temperature field and grinding quality using dry grinding and established a mathematical model. Gao et al. [10] compared wet grinding with dry grinding of CFRP by introducing carbon nanotube-based biolubricants, and found that wet grinding yields better grinding effects. While numerous studies have investigated the processing of CFRP using these methods, grinding has garnered significant interest due to its simplicity, ease of operation, and lower propensity to produce fiber pull-out defects.

The cutting tools commonly used in carbon fiber grinding are grinding wheels [11–13]. Wen et al. [14] studied the relationship and mechanism between grinding force and various parameters in grinding carbon fiber reinforced polymer (CFRP). They pointed out that grinding force is positively correlated with grinding depth and feed rate, while negatively correlated with wheel speed. This provides theoretical guidance for future research on the relationship between grinding force and temperature, as well as the degree of clogging in grinding. Geng et al. [15] used a diamond grinding tool to machine grooves under dry conditions and found that rotary ultrasonic elliptical machining can effectively reduce cutting forces and prolong tool life compared to conventional machining methods. Cong et al. [16] studied the power consumption of an ultrasonic system under constant-speed grinding, providing a good processing solution for CFRP grinding.

In recent years, researchers have used grinding methods to analyze and study the fracture of fibers in CFRP under microscopic conditions, expanding the grinding mechanism of CFRP. Ning et al. [17] use rotary ultrasonic machining to process CFRP. By studying the mechanism of fiber material removal during single particle scratching, the interrelationship between fiber peeling and fracture was revealed. It provided ideas for studying the cutting action of multiple abrasive grains on CFRP in the future. In addition, Voss et al. [18] developed a model for fiber fracture under grinding, while Wei et al. [19] investigated the grinding removal mechanism of single grain on long fiber reinforced braided composites, and the effect of fiber orientation on grinding force. Yin et al. [20] studied the removal mechanism of grinding machining SiCf/SiC porous materials, while Liu et al. [21] developed a model for grinding removal and fiber fracture of two-dimensional C/SiC materials. The study of micro mechanisms can establish the relationship between processing technology and mechanism, optimize process plans, and improve processing efficiency. Kodama et al. [13] analyzed the effect of dry grinding and wet grinding on the grinding quality in grinding CFRP based on a grinding machine, and suggested that wet grinding can effectively improve the grinding quality of CFRP. The use of coolant in mechanical processing not only reduces the temperature of the tool but also facilitates chip evacuation, making it a good choice for improving processing efficiency and quality. Handa et al. [12] developed a heating model for eccentric sleeve grinding (ESG) of CFRP, and ESG was found to improve the quality of CFRP grinding compared with conventional grinding methods. The combination of this model and ABAQUS can predict the optimal parameters to ensure grinding quality. It is possible to reduce unnecessary operations in production. Esmaeili et al. [22] developed a three-dimensional roughness model to reflect the effect of the grinding process and analyzed the effects of wetting, feed rate, and grinding depth on the quality of the grinding process to provide appropriate machining strategies. Handa et al. [23] proposed an eccentric sleeve grinding strategy for CFRP, which reduces or eliminates scallop like marks on the grinding surface by changing the motion trajectory of the grinding tool. And by combining the morphology and quality of CFRP at the micro level, grinding parameters were adjusted to achieve higher quality grinding surfaces. The combination and analysis of the model provided strong data support for the experiment. Moreover, in recent years, some researchers have been collecting and analyzing acceleration signals of CFRP during the cutting process, and applying them for predictive analysis of machining quality and tool wear [24, 25]. However, there is still limited research on the relationship between the transformation of acceleration signals and the corresponding cutting mechanisms in the cutting process of CFRP.

The purpose of this study is to analyze the influence of grinding angle on the acceleration signal during the grinding process and the analysis of grinding quality. By analyzing the changes in acceleration vibration frequency and amplitude during the initial, middle, and final stages of grinding, the removal mechanism of CFRP and the analysis of fiber fracture are studied.

2 Experimental

2.1 Materials

A workpiece of carbon fiber reinforced polymers (CFRP) was fabricated from TORAY USN150A Prepreg. The prepreg is laid in the full 0° and cured for 1.5 hours at 175°C under a pressure of 2 MPa. The resulting laminate had dimensions of 200 mm×20 mm and a thickness of 2 mm. Laminate specimens with desired fiber orientations were cut for subsequent grinding experiments. The mechanical properties of the CFRP are listed in Table 1.

2.2 Equipment and Grinding

The CFRP grinding platform used is shown in Figure 1. It comprised of a FANUC M20id industrial robot, a 3-D workbench, an acceleration sensor, a diamond grinding

Table 1 Mechanical properties of the CFRP material

Carbon fiber	**TORAY USN150A Prepreg**	
Matrix	Thermosetting epoxy resin	
Fiber content	54 vol%	
Molding process	Mold forming	
Fiber angle (deg)	**Tensile strength (MPa)**	**Young's Modulus (GPa)**
0	2600	128
90	1335	–

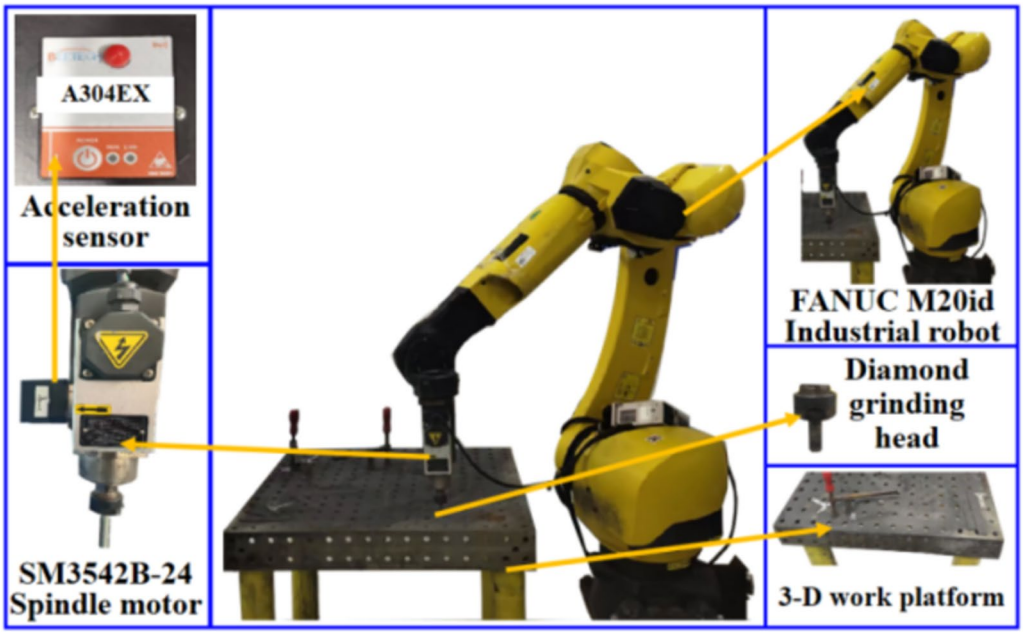


Figure 1 The CFRP grinding platform

head, and an SM3542B-24 spindle motor. The grinding process is illustrated in Figure 2a, where the grinding head rotates counter-clockwise. The x-axis was defined as the short side of the sample strip, the y-axis as the long side of the strip, and the z-axis as the vertical machining plane direction. The grinding direction angle is defined as the angle between the counter-clockwise rotated grinding head's feed direction and the 0° fiber orientation. The coolant used during grinding is distilled water.

The process's configuration parameters significantly impact the experimental outcomes. Wang et al. [26] investigated the influence of various process parameters on the surface quality of CFRP in industrial robot grinding. Hence, to investigate the relationship between acceleration signals and grinding mechanisms during the grinding process of industrial robots, a systematic study was conducted on the grinding mechanism using the parameters shown in Table 2 below. Before starting the grinding process, secure the CFRP using a fixture on the 3D workbench. Three areas were selected in the grinding area and measured with the flatness measuring instrument (HNJL8630), and the values were all kept below 0.05. The samples after grinding in different directions are shown in Figure 2b.

2.3 Analysis Methods

Vibration signals during grinding processes can provide valuable insights according to previous studies [27–29]. Kong et al. [30] investigated the influence of grinding parameters on the temperature of the workpiece and the processing vibration signal in the study of grinding strengthening technology, aiming to explore

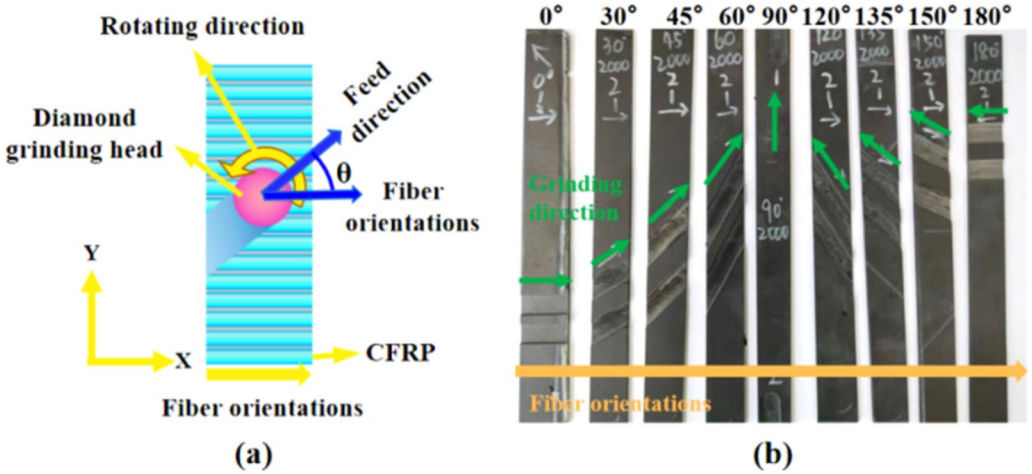


Figure 2 Grinding parameter diagram: (**a**) Schematic of grinding process, (**b**) The sample after grinding

Table 2 CFRP grinding experimental parameters

Parameters	Value
Grinding direction angle (θ)	0°, 30°, 45°, 60°, 90°, 120°, 135°, 150°, 180°
Rotating speed	4000 r/min
Mesh size of griding head	#80
Feed speed	4 mm/s
Grinding depth	1 mm
Grinding width	10 mm

the correlation between the strengthening layer and the vibration signal. Guo et al. [31] used acoustic emission signals and vibration signals to process the signal features using machine learning, providing feasibility for predicting the quality of grinding surfaces. To investigate the mechanism of grinding based on industrial robots, acceleration data were collected during the grinding process. The acceleration data reflect the trend of relative motion between the grinding head and the sample surface, and can provide an analysis of the vibration of the grinding head and thus the mechanism of action of the grinding head in grinding CFRP.

During the grinding process, acceleration data is recorded in real-time mode, and the Fast Fourier Transform (FFT) method commonly used in vibration analysis is employed to convert the time-domain signal in the *Z*-axis direction into a frequency-domain signal (see Figure 3). From the time-domain variation graph of acceleration, it can be observed that there are significant periodic changes before and after grinding. This is attributed to factors such as uneven contact between the grinding head and work piece, as well as non-uniformity in the internal structure of the work piece. Therefore, based on the time-domain variation of acceleration during the grinding process, the entire process is divided into three stages: the beginning, middle, and end of grinding. The acceleration time-domain signals of these three stages are then transformed into acceleration frequency-domain signals.

In addition, microscopic pictures, three-dimensional morphology images, and three-dimensional contours of the CFRP surface were collected, and Scanning Electron Microscopy (SEM) was used to photograph the microscopic morphology of the samples. Combined with the acceleration signal and microscopic morphological changes, the mechanism of CFRP grinding and removal was analysed.

3 Results and Discussion

3.1 The Relationship between Grinding Angle and Acceleration Vibration Signal

When the grinding angle increases from 0° to 90°, the fiber fracture mode changes from micro-flexure fracture to bending fracture and then to compression fracture; when the grinding angle increases from 90° to 180°, the fiber fracture mode changes from compression fracture to bending fracture and then to micro-flexure fracture. The schematic diagram of the change in fiber breakage mode is shown in Figure 4.

As shown in Figure 5, When the grinding angle changes, the vibration frequency and energy generated during grinding are mainly concentrated around 200 Hz, which is the main vibration mode of CFRP grinding removal. When the grinding direction is 0°–90°, the *Z*-axis acceleration time-domain diagram and FFT diagram during the overall grinding process are shown in Figure 5. The results show that the maximum amplitude increases with the increase in grinding direction (from

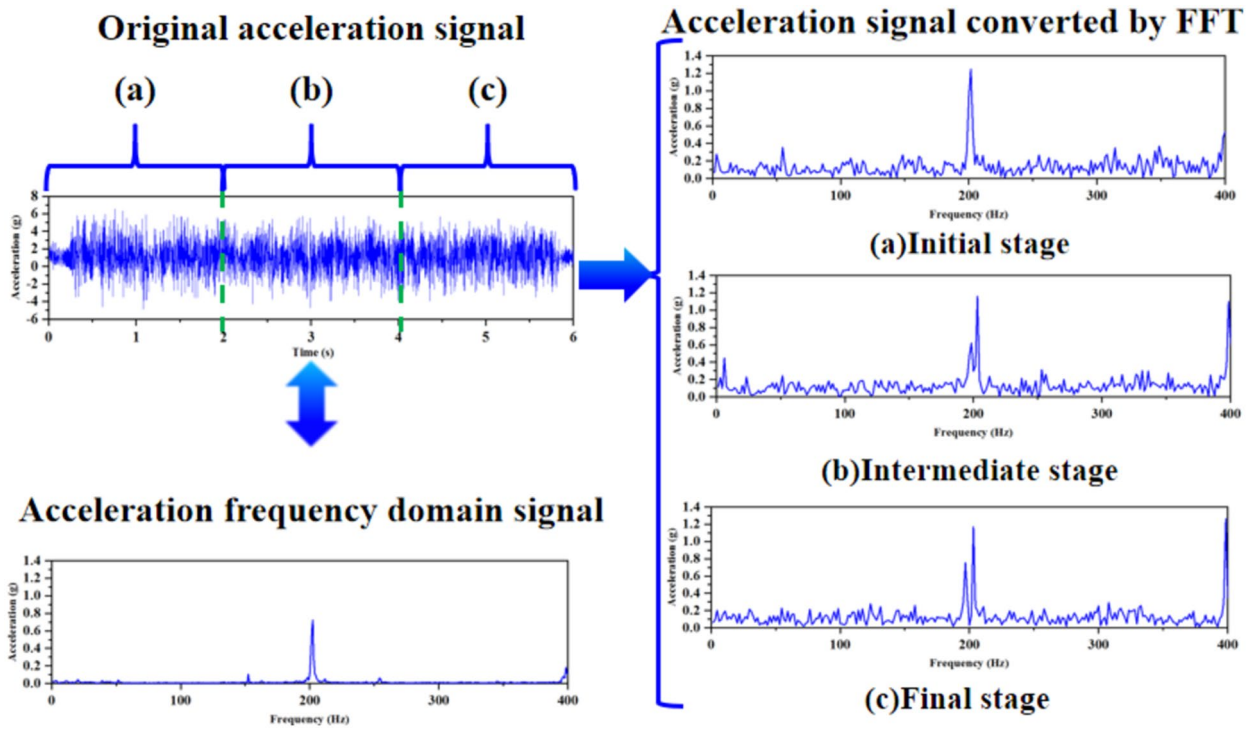


Figure 3 FFT diagram of three stages in acceleration time domain

0.164 to 0.211 g). The maximum acceleration decreases at 60° (0.173 g), which is consistent with Ref. [18] which also showed that the flexural strength of fiber decreases at a grinding direction of 60°. During the transition from 0° to 90°, the fiber fracture mode changes from bending fracture to compression fracture, which leads to an increase in grinding resistance and eventually an increase in acceleration amplitude. As can be seen from Figure 4(a), when the grinding Angle is 0°, the strength of the fiber direction is high, while the strength of the connection between the fiber and the matrix is weak. Therefore, in the feed direction of grinding, the fiber is separated from the substrate under the action of pressure and produces a micro-bending fracture. The fibers on both sides of the grinding head produce elastic bending deformation under debris and extrusion of the grinding head. Due to the interlayer gap between the fiber layer at the bottom of the grinding head and the upper fiber, the amplitude of acceleration vibration in Figure 5a is small. As the grinding Angle increases, the fibers above the feed of the grinding head bend under the action of extrusion, and eventually lead to fracture. As the unground fiber layer impedes the bending of the grinding head, the resistance increases along the *Y* direction, resulting in an increase in the maximum amplitude of the acceleration. The fiber in the lower right direction fed by the grinding head is subjected to less pressure, and only slight bending deformation occurs. When the grinding Angle is 60°, the fiber above the grinding head is compressed and bends and breaks. However, the pressure on the lower right of the fiber fed by the grinding head gradually increases, and the bending deformation exceeds the maximum strength of the fiber. Therefore, as shown in Figure 4e, bending micro-cracks occur. With the grinding process, the micro-cracks expand until they extend to the connection surface between the fiber and the resin matrix and turn into interlayer cracks, which rapidly reduces the resistance and thus the acceleration vibration amplitude. When the grinding Angle is 90°, the fibers above the feed direction of the grinding head will compress and break, because the fibers that have not been ground will have the greatest fiber obstruction at the deformation site. When the grinding Angle increases from 90° to 180°, the fiber changes from a compression fracture to bending fracture and finally to slightly bending fracture, and the fracture mechanism is the same as 0° to 90°.

The graph in Figure 6 shows the maximum vibration peaks of acceleration in the initial stage, intermediate stage and final stage of grinding. At the beginning of the grinding process, a larger amplitude is generated. As the grinding progresses, the amplitude gradually decreases. However, towards the end of the grinding process, the amplitude slightly increases. This is because at the beginning of grinding, the uneven contact between the

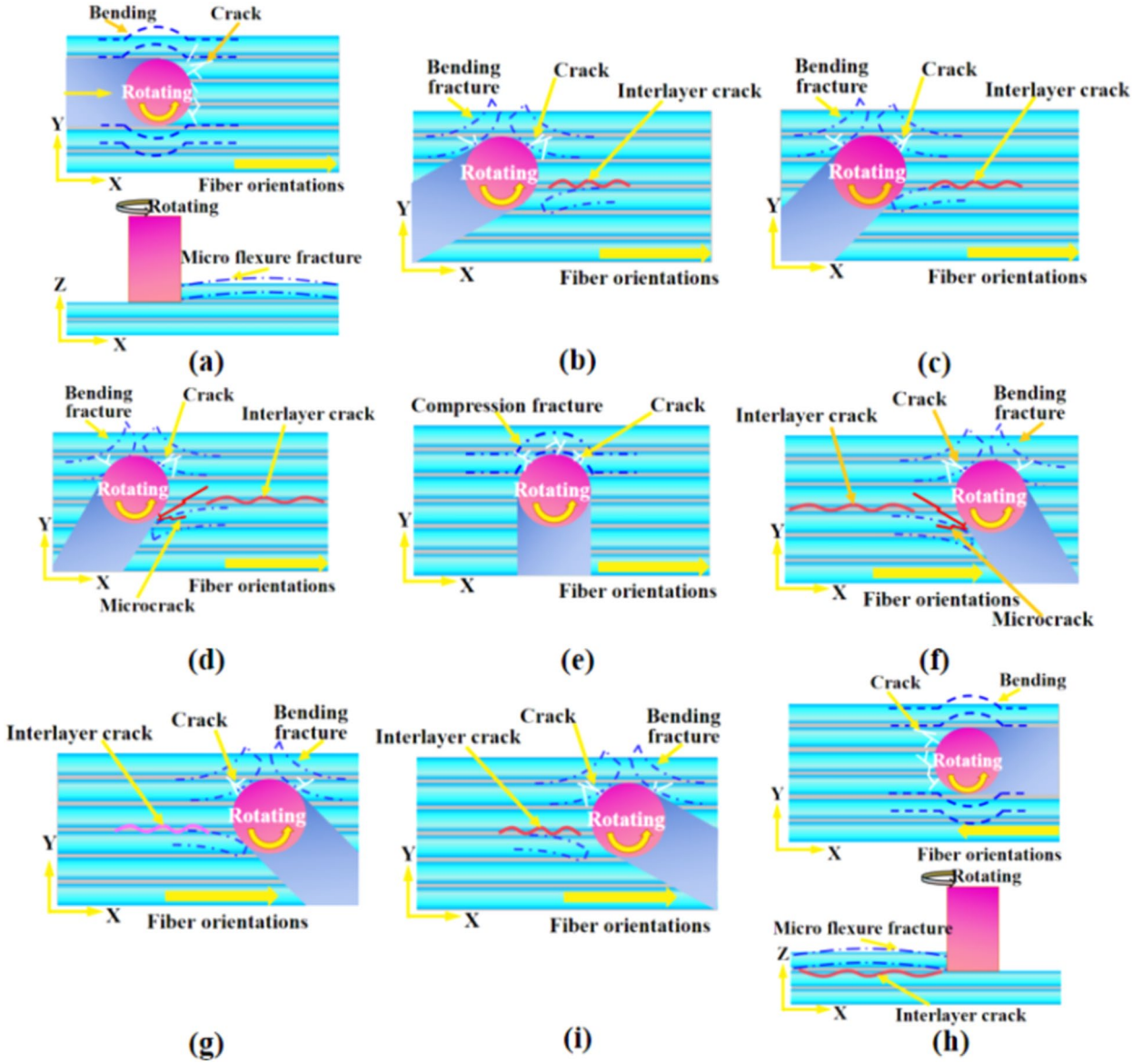


Figure 4 The schematic diagram of the change in fiber breakage mode: **a** 0°, **b** 30°, **c** 45°, **d** 60°, **e** 90°, **f** 120°, **g** 135°, **h** 150°, **i** 180°

processed surface and the grinding head, coupled with an increase in grinding debris as the grinding amount increases, results in increased resistance and grinding force, which is the interaction force between the workpiece and the grinding head. Therefore, a larger amplitude is generated at the beginning of the grinding process. In the intermediate stage of grinding, the cutting amount remains constant and the resistance does not vary significantly, resulting in a smaller amplitude. When the grinding process approaches completion and the grinding amount suddenly decreases, there is a significant change in resistance, causing unstable and increased amplitude.

3.2 Grinding Mechanism of Micro Morphology Changing with Grinding Angle

Under different grinding angles, the co-focusing microscopic images of surface roughness in the three stages are shown in Figure 7. It can be observed that the size of the red area at the beginning and end of grinding is larger than that in the middle. This is because the amplitude in the Z-axis direction is larger at the initial and final stages of grinding compared to the intermediate stage. Excessive amplitude causes the grinding head to continuously vibrate in the Z-axis direction, resulting in surface roughness due to impact on the processed surface. Further evidence of the higher surface quality in

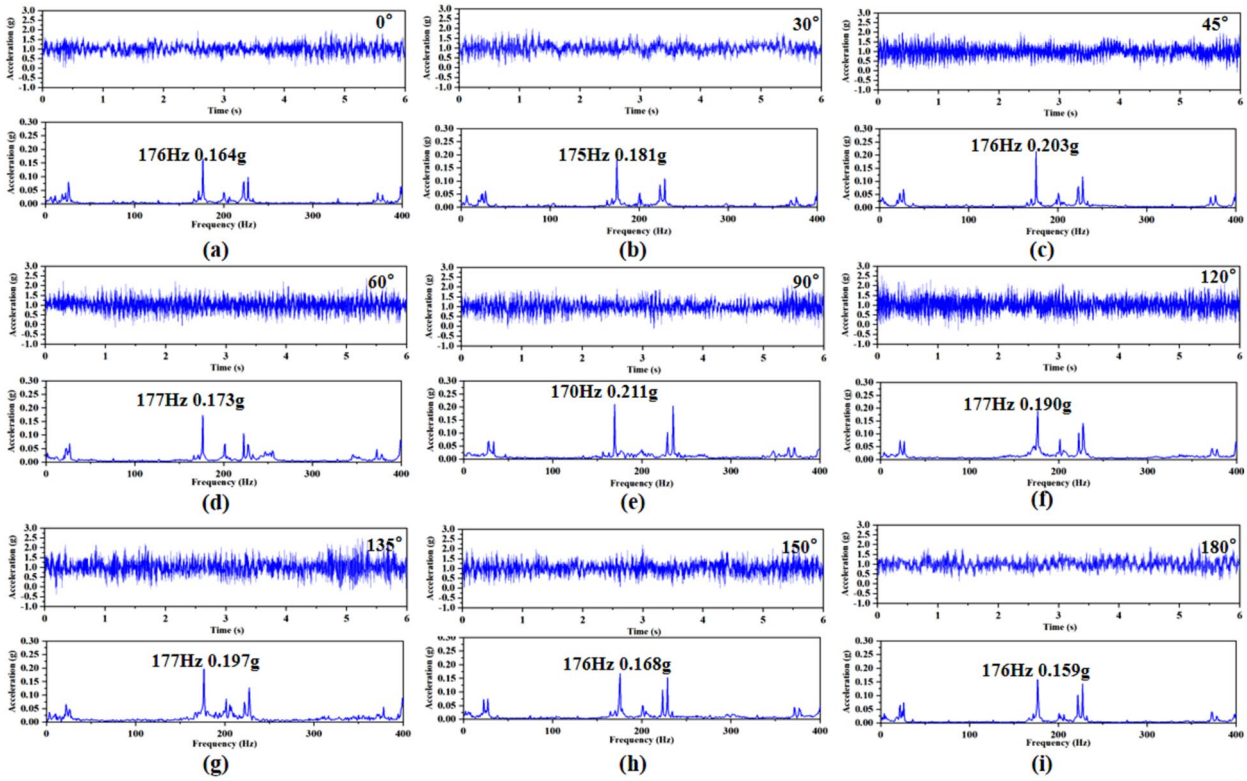


Figure 5 *Z*-axis acceleration diagram by FFT: **a** 0°, **b** 30°, **c** 45°, **d** 60°, **e** 90°, **f** 120°, **g** 135°, **h** 150°, **i** 180°

the middle section compared to the beginning and end is demonstrated by the variation of roughness within the three grinding stages, as shown in Figure 8. Additionally, there is a strong correlation between the roughness of the processed surface and the amplitude of acceleration. The larger the amplitude, the rougher the surface quality. With an increase in the grinding angle, the maximum amplitude of acceleration increases first and then decreases. The variation in roughness in the three stages also has the same trend. When the fiber angle is 90°, the fibers undergo compression and fracture by the grinding head, resulting in higher grinding resistance. As a result, higher amplitudes are generated in all three stages of grinding, leading to a decrease in surface quality. Comparing Figure 6 and Figure 8, it is evident that the trend of surface roughness after grinding corresponds to the variation trend of the maximum vibration peak in the acceleration frequency domain. Therefore, subsequent adjustments can be made to various factors during processing to control the vibration amplitude of acceleration, thereby improving surface quality.

In the grinding process, different grinding stages correspond to different grinding surface morphologies. Here, observations were made at a grinding angle of 0°. Figure 9 shows the grinding mechanism at a 0° grinding angle, while Figure 10 shows the microscopic morphology at each stage. In the initial stage of grinding, the side of the diamond grinding head initially comes into contact with CFRP. Under pressure, CFRP undergoes elastic deformation, causing the lower layer of the bottom edge of the diamond grinding head to bend upward and form warping. As grinding progresses, the material removal rate increases. The diamond grinding head vibrates violently up and down in the direction of *Z* axis, and the fiber is subjected to pressure and vibration to produce microbending deformation and cracks. As the grinding progresses, the fiber breaks and is stripped from the resin. The shear force is greater than the interlayer strength, and the warping resistance of the lower CFRP at the bottom edge of the diamond grinding head is released. The lower CFRP then recovers to its original condition under the action of elasticity. In the initial stage of grinding, the cutting mode is constantly repeated, thus leading to a growing grinding resistance and consequent formation of ripples on the grinding surface. Therefore, as shown in Figure 9a, uneven cutting and collisions occur at the point of initial contact between the grinding tool and the carbon fiber, resulting in a wavy pattern with unevenness on the ground surface. As the grinding continues, the state of the grinding tool stabilizes, and the vibration

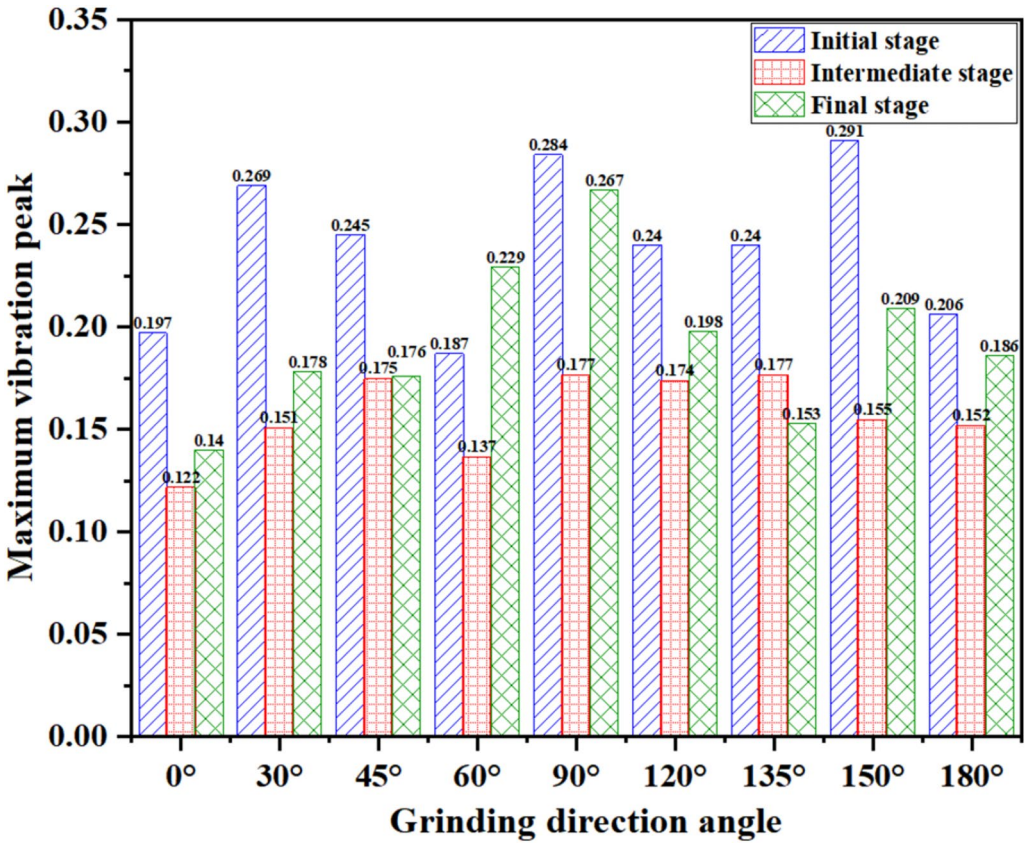


Figure 6 Maximum vibration peak of acceleration frequency domain the initial stage, intermediate stage and final stage

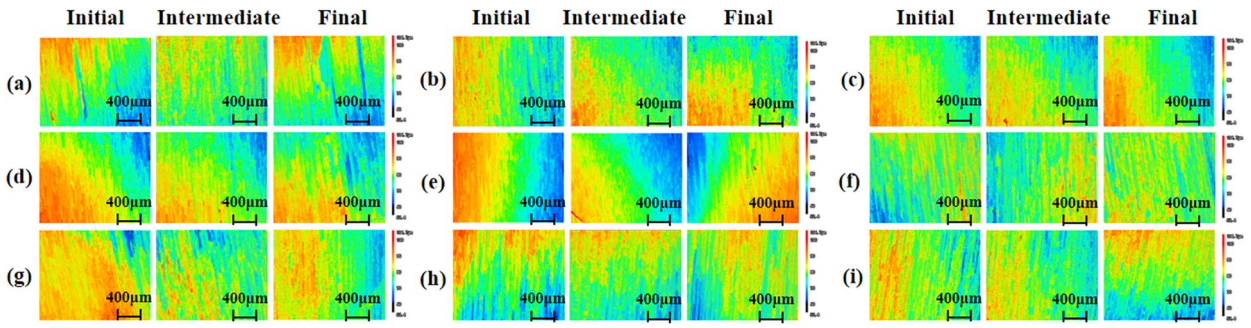


Figure 7 Confocal microscope images of the initial stage, the intermediate stage and the final stage under different angles: **a** 0°, **b** 30°, **c** 45°, **d** 60°, **e** 90°, **f** 120°, **g** 135°, **h** 150°, **i** 180°

peaks of the grinding acceleration become smaller. As shown in Figure 9b, as the grinding process continues, the fibers at the contact point in the feed direction are subjected to pressure due to the initial contact of the side of the diamond grinding head with the CFRP. As the pressure gradually increases, the shear force between the upper fibers and the resin matrix exceeds the maximum value, causing interlayer cracks to propagate and the fibers to undergo micro-bending fracture. Meanwhile, the end face of the diamond grinding head exerts downward pressure and friction on the fibers on the grinding surface. Under the action of vibration, the fibers are peeled off from the resin, forming pits due to fiber pulling. During the final stage of grinding, the amount of grinding decreases and the contact area gradually decreases. Unstable grinding vibrations result in a large

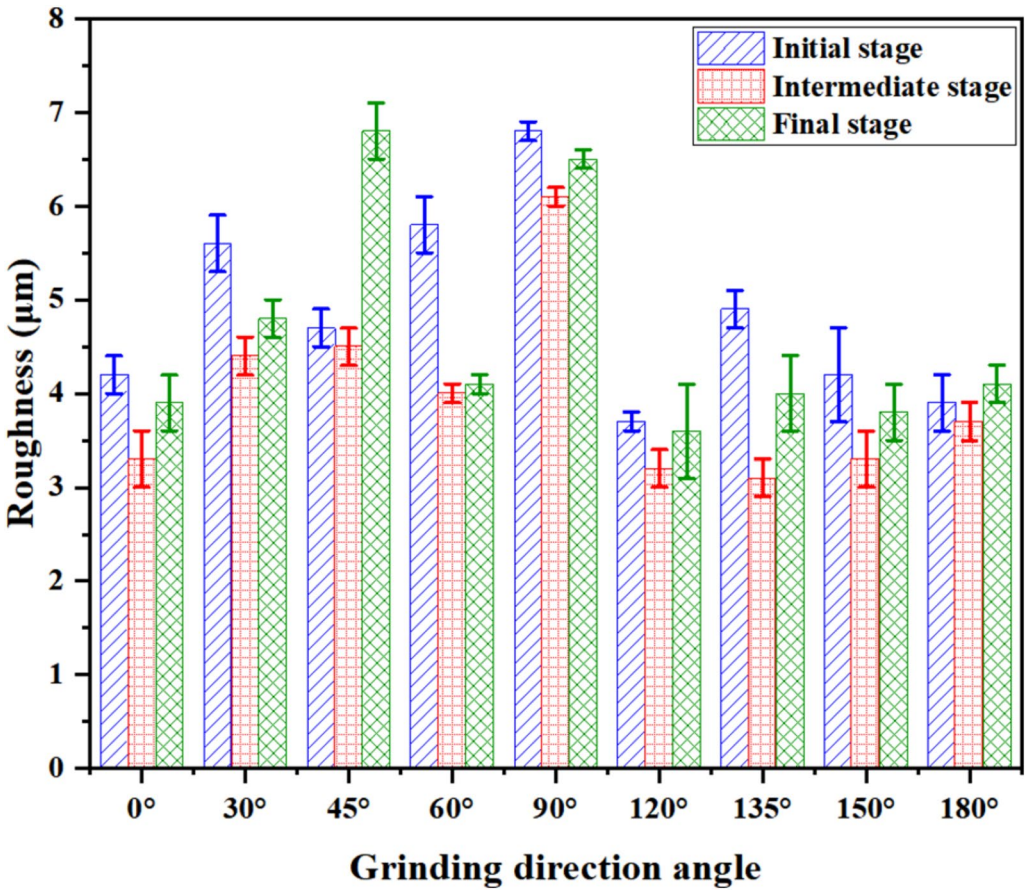


Figure 8 Changes in roughness in the initial stage, intermediate stage and final stage under different angles

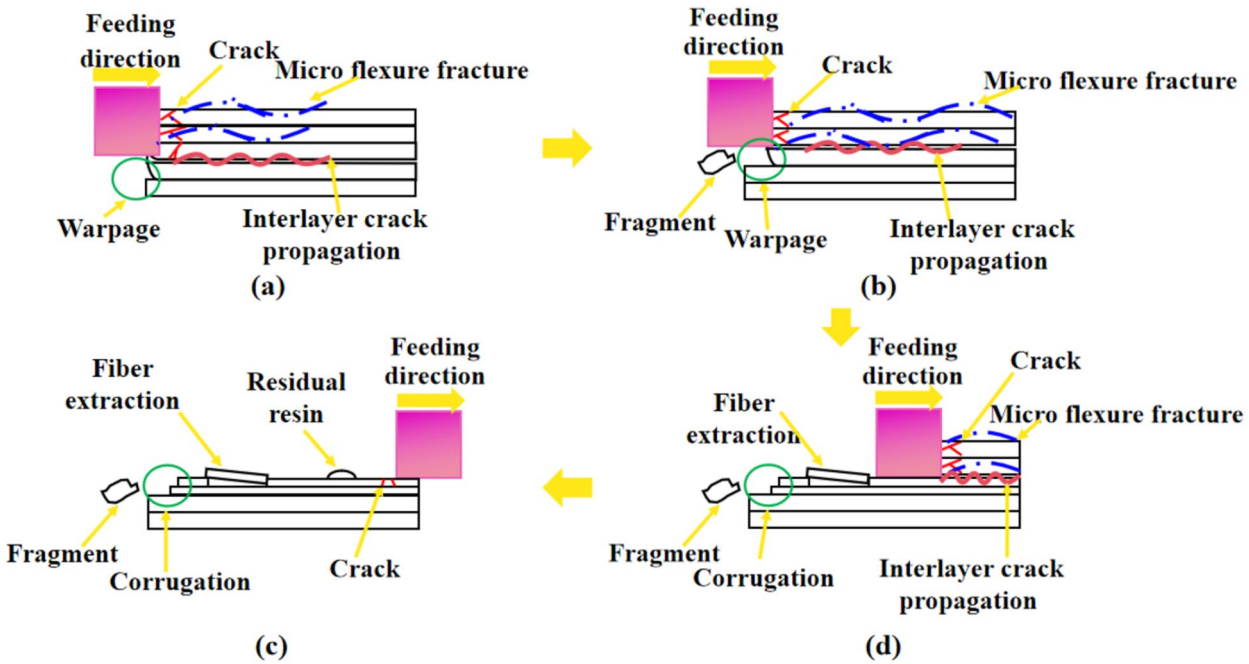


Figure 9 Schematic diagram of grinding mechanism: **a, b** Initial stage, **c** The intermediate stage, **d** Final stage

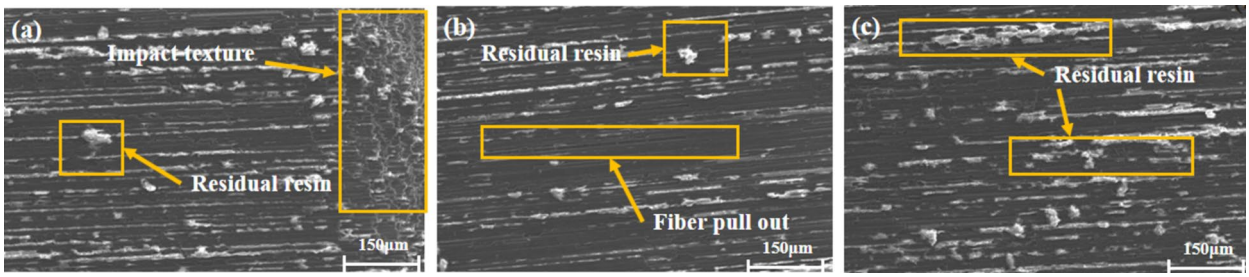


Figure 10 SEM: **a** Initial stage, **b** The intermediate stage, **c** Final stage

amount of resin and peeled fibers remaining on the surface of the ground fibers.

When grinding enters the mid-stage, the grinding process becomes more stable. From the graph in Figure 11, it can be observed that there is less resin and fiber residue after grinding. At a grinding angle of 0°, fibers exhibit a slightly curved fracture, mainly peeling off from the resin, resulting in intact fibers on the ground surface after grinding. When the grinding angle ranges from 0° to 60°, as the angle increases, the fibers transition from slightly curved fractures to curved fractures. Fibers can be seen bending and fracturing in the direction of grinding, resulting in uneven fracture surfaces. As the grinding angle increases, grinding resistance also increases, leading to greater vibration amplitude of the grinding head, causing intact fibers to bend and fracture into smaller segments, increasing the number of fiber segments and remaining resin. At a grinding angle of 90°, fibers exhibit compression fracture, and the ground fibers show a smoother fracture

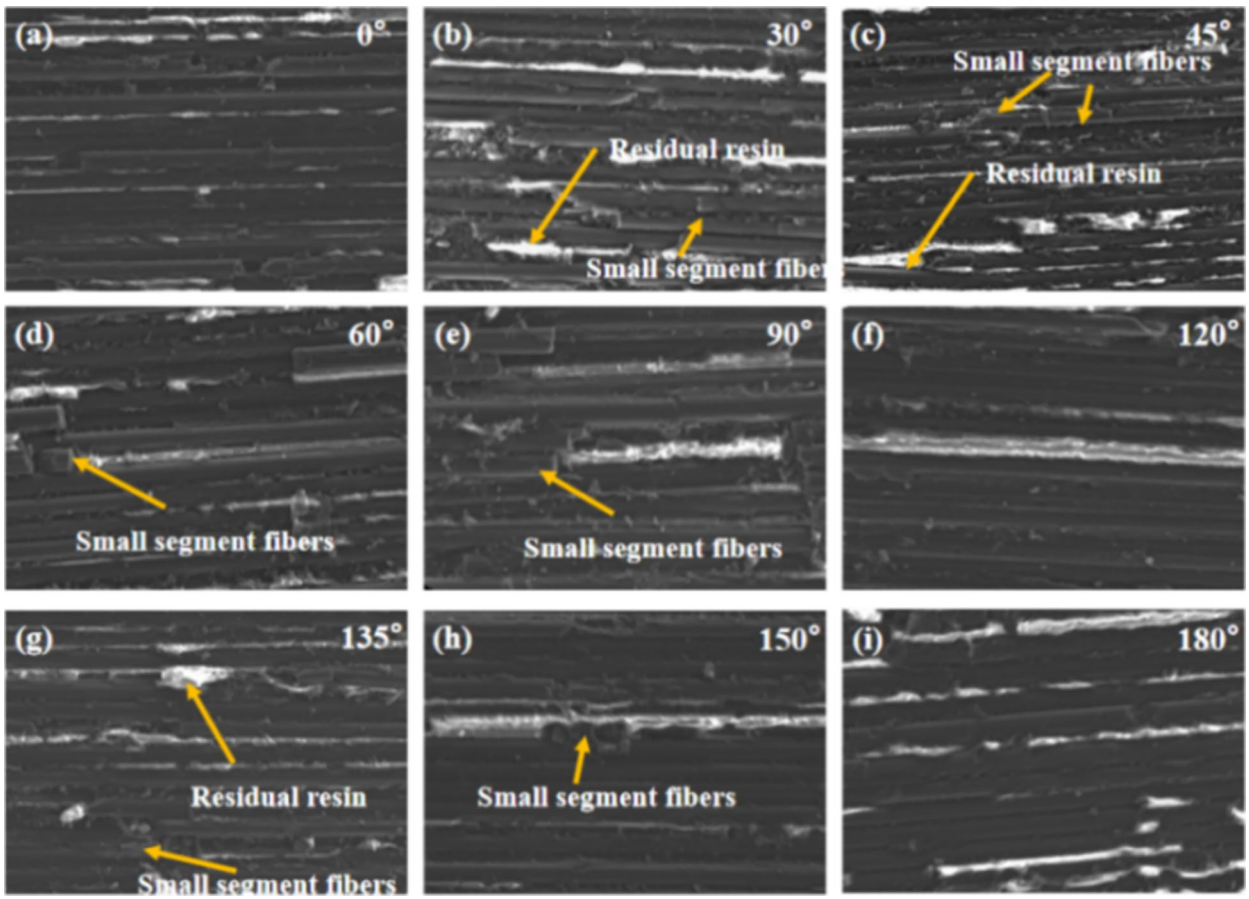


Figure 11 SEM images of the intermediate stage: **a** 0°, **b** 30°, **c** 45°, **d** 60°, **e** 90°, **f** 120°, **g** 135°, **h** 150°, **i** 180°

surface. When the grinding angle ranges from 120° to 180°, as the angle increases, fibers transition from curved fractures to slightly curved fractures. As the angle increases, grinding resistance decreases, reducing the vibration amplitude of the grinding head, allowing intact fibers to remain more prevalent with a decrease in remaining resin.

4 Conclusions

The present study adopts the approach of analyzing acceleration signals combined with micrograph images to investigate the mechanisms of the entire grinding process and different grinding stages. The conclusions are as follows:

- In the grinding process, the maximum vibration peak and roughness of acceleration frequency domain signal increase first and then decrease with the increase of grinding angle. For grinding angles of 60° and 120°, the expansion of microcracks reduces the feed resistance of the grinding head, leading to smaller amplitudes and a decrease in roughness.
- Compared to the initial and final stages, the acceleration amplitude during the middle stage of grinding is lower, resulting in a lower surface roughness after grinding.
- When the grinding angle changes from 0° to 90°, the fracture of the carbon fiber tends to be small and short, and there is a large amount of residual resin. When the grinding angle is extended from 90° to 180°, the fiber fracture tends to break away from the resin, and the amount of residual resin is reduced.

The relationship between the variation of acceleration signals and surface quality at each stage of the grinding process is investigated, providing data support for CFRP grinding. Furthermore, subsequent experiments are required to establish a relational model, enabling real-time monitoring of acceleration signal changes to enhance machining accuracy.

Acknowledgements
Not applicable.

Author Contributions
LC conducted relevant experiments to analyze the relationship between acceleration signal changes and angles, and wrote the paper. FY conducted relevant experiments and clarified the rules. PD and SS made relevant graphs and processed the data. KJ, LC, GB, and LQ reviewed and revised the article. All authors read and approved the final manuscript.

Funding
Supported by the Qingdao Municipal Natural Science Foundation (Grant No. 23-2-1-246-zyyd-jch) and Lianyungang Municipal Key Research and Development Plan (Grant No.CG2310).

Declarations

Competing Interests
The authors declare no competing financial interests.

Received: 20 March 2024 Revised: 24 October 2024 Accepted: 4 November 2024
Published online: 26 December 2024

References

[1] A. Al-Lami, P. Hilmer, M. Sinapius. Eco-efficiency assessment of manufacturing carbon fiber reinforced polymers (CFRP) in aerospace industry. *Aerospace Science and Technology*, 2018, 79: 669-678.
[2] O. Dababneh, T. Kipouros. A review of aircraft wing mass estimation methods. *Aerospace Science and Technology*, 2018, 72: 256-266.
[3] Y. Sun, Z. B. Cai, S. B. Wu, et al. Effect of cycling low velocity impact on mechanical and wear properties of CFRP laminate composites. *Chinese Journal of Mechanical Engineering*, 2018, 31(1): 10.
[4] H. T. Liu, J. Lin, Y. Z. Sun, et al. Micro model of carbon fiber/cyanate ester composites and analysis of machining damage mechanism. *Chinese Journal of Mechanical Engineering*, 2019, 32 (1): 11.
[5] S. Guo, W. Du, Q. H. Jiang, et al. Surface integrity of ultrasonically-assisted milled Ti6Al4V alloy manufactured by selective laser melting. *Chinese Journal of Mechanical Engineering*, 2021, 34 (1): 14.
[6] Z. C. Yang, L. D. Zhu, G. X. Zhang, et al. Review of ultrasonic vibration-assisted machining in advanced materials. *International Journal of Machine Tools & Manufacture*, 2020, 156 34.
[7] Z. D. Li, X. B. Wang and B. Zhao. An experiment study on milling forces in the ultrasonic milling of CFRP. *3rd International Conference on Manufacturing Science and Engineering (ICMSE 2012)*, Xiamen, China, 2012: 1028-1031.
[8] R. Balaji, S. Sivakumar, M. Nadarajan, et al. A recent investigations: Effect of surface grinding on CFRP using rotary ultrasonic machining. *9th International Conference of Materials Processing and Characterization (ICMPC)*, Gokaraju Rangaraju Inst Engn & Technol, Hyderabad, India, 2019: 5209-5218.
[9] H. Gao, H. L. Ma, Y. J. Bao, et al. Theoretical analysis of grinding temperature field for carbon fiber reinforced plastics. *13th International Symposium on Advances in Abrasive Technology/1st Cross-Strait Conference on Precision Machining*, Taipei, China, 2010: 52-57.
[10] T. Gao, Y. B. Zhang, C. H. Li, et al. Grindability of carbon fiber reinforced polymer using CNT biological lubricant. *Scientific Reports*, 2021, 11(1): 14.
[11] J. C. Tian, R. K. Kang, Z. G. Dong, et al. Multi-scale machining damages of CFRP circular cell honeycomb during end face machining. *Journal of Manufacturing Processes*, 2023, 86: 282-293.
[12] D. Handa, V. S. Sooraj. Thermal investigations on eccentric sleeve grinding of fibre reinforced composites. *Journal of Manufacturing Processes*, 2022, 84: 1404-1427.
[13] H. Kodama, S. Okazaki, Y. F. Jiang, et al. Thermal influence on surface layer of carbon fiber reinforced plastic (CFRP) in grinding. *Precision Engineering-Journal of the International Societies for Precision Engineering and Nanotechnology*, 2020, 65: 53-63.
[14] Z. H. Wen, H. Zhao, X. Yan, et al. Grinding performance study of CF/epoxy and CF/PEEK composites. *Polymer Composites*, 2023, 44(8): 4565-4578.
[15] D. X. Geng, D. Y. Zhang, Y. G. Xu, et al. Rotary ultrasonic elliptical machining for side milling of CFRP: Tool performance and surface integrity. *Ultrasonics*, 2015, 59: 128-137.
[16] W. L. Cong, Z. J. Pei, T. W. Deines, et al. Rotary ultrasonic machining of CFRP composites: A study on power consumption. *Ultrasonics*, 2012, 52(8): 1030-1037.
[17] F. D. Ning, H. Wang, W. L. Cong. Rotary ultrasonic machining of carbon fiber reinforced plastic composites: a study on fiber material removal mechanism through single-grain scratching. *International Journal of Advanced Manufacturing Technology*, 2019, 103 (1-4): 1095-1104.
[18] R. Voss, L. Seeholzer, F. Kuster, et al. Analytical force model for orthogonal machining of unidirectional carbon fibre reinforced polymers (CFRP) as a function of the fibre orientation. *Journal of Materials Processing Technology*, 2019, 263 440-469.

[19] J. H. Wei, H. J. Wang, B. Lin, et al. A force model in single grain grinding of long fiber reinforced woven composite. *International Journal of Advanced Manufacturing Technology*, 2019, 100(1-4): 541-552.
[20] J. F. Yin, J. H. Xu, W. F. Ding, et al. Effects of grinding speed on the material removal mechanism in single grain grinding of SiCf/SiC ceramic matrix composite. *Ceramics International*, 2021, 47 (9): 8.
[21] Q. Liu, G. Q. Huang, X. P. Xu, et al. A study on the surface grinding of 2D C/SiC composites. *International Journal of Advanced Manufacturing Technology*, 2017, 93(5-8): 1595-1603.
[22] H. Esmaeili, H. Adibi, S. M. Rezaei. An efficient strategy for grinding carbon fiber-reinforced silicon carbide composite using minimum quantity lubricant. *Ceramics International*, 2019, 45(8): 10852-10864.
[23] D. Handa, V. S. Sooraj. An eccentric sleeve grinding strategy for fibre-reinforced composites. *Composites Part B-Engineering*, 2019, 176: 13.
[24] G. Q. Zhu, S. S. Hu, H. Q. Tang. Prediction of tool wear in CFRP drilling based on neural network with multicharacteristics and multisignal sources. *Composites and Advanced Materials*, 2021, 30: 15.
[25] J. Zhou, X. Y. Mao, H. Q. Liu, et al. Prediction of cutting force in milling process using vibration signals of machine tool. *International Journal of Advanced Manufacturing Technology*, 2018, 99 (1-4): 965-984.
[26] F. Y. Wang, S. Y. Xuan, Z. Y. Chang, et al. Effect of grinding parameters on industrial robot grinding of CFRP and defect formation mechanism. *International Journal of Precision Engineering and Manufacturing-Green Technology*, 2024, 11(2): 427-438.
[27] W. Z. Huang, Y. Li, X. Wu, et al. The wear detection of mill-grinding tool based on acoustic emission sensor. *International Journal of Advanced Manufacturing Technology*, 2023, 124(11-12): 4121-4130.
[28] C. H. Lee, J. S. Jwo, H. Y. Hsieh, et al. An intelligent system for grinding wheel condition monitoring based on machining sound and deep learning. *IEEE Access*, 2020, 8: 58279-58289.
[29] E. A. Dias, F. B. Pereira, S. L. Ribeiro, et al. Monitoring of through-feed centreless grinding processes with acoustic emission signals. *Measurement*, 2016, 94:71-79.
[30] X. N. Kong, S. C. Xiu, C. Sun, et al. Study on the relevance of strengthened layer and vibration signal in grinding-strengthening process. *International Journal of Advanced Manufacturing Technology*, 2022, 121(11-12): 7963-7982.
[31] W. C. Guo, C. J. Wu, Z. S. Ding, et al. Prediction of surface roughness based on a hybrid feature selection method and long short-term memory network in grinding. *International Journal of Advanced Manufacturing Technology,* 2021, 112(9-10): 2853-2871.

Lichen Li born in 1999, is currently a master's student at the *College of Materials Science and Engineering, Ocean University of China*. His main research focuses on the processing of composite materials in industrial robot applications, machine learning, and the simulation of composite materials.

Fangyuan Wang born in 1996, is currently a researcher at the *Commercial Aircraft Corporation of China, Ltd*. He obtained his master's degree from *Ocean University of China* and his bachelor's degree from *Southeast University, China*. His research interests include the processing of composite materials in industrial robot applications and machine learning.

Pengda Song born in 1999, received his master's degree from *Ocean University of China* and his bachelor's degree from *Harbin Institute of Technology, China*. He mainly studies the processing control technology of composite molding processes, optimization of repair process parameters based on deep learning techniques, and visual recognition and texture analysis of CFRP grinding surface quality through machine vision.

Kai Jin born in 1987, is currently a professor at the *College of Materials Science and Engineering, Ocean University of China*. He obtained his bachelor's degree from *Harbin Institute of Technology, China,* and his doctoral degree from *Sogang University, Republic of Korea*, where he served as a distinguished researcher (postdoctoral). He has long engaged in the intelligent design and repair of structural composite materials, as well as the preparation of multi-energy field resin-based composites.

Lei Chu born in 1977, is currently a lecturer at *Ocean University of China*. Her main research direction is in functional materials and composite materials.

Sansan Ding born in 1967, is the Deputy Chief Engineer of *CRRC Qingdao Sifang Co., Ltd*., *China*, and the deputy secretary of the *Party Committee of the National Engineering Laboratory (Engineering Research Center), China*. Additionally, he is the director of the *National Engineering Research Center, China* and the executive deputy director of the *National Engineering Laboratory, China*, as well as a scientist at CRRC.

Guido A. Berti born in 1960, is currently a professor in the *Department of Management and Engineering*, *University of Padua, Italy,* and the *United Nations Development Programme, Italy*. His main research focuses on machine learning and simulation of composite materials.

Luca Quagliato born in 1987, is currently a professor at *Ewha Womans University, Republic of Korea*. His research directions include FRP and composite materials, the application of machine learning in design and manufacturing, additive manufacturing, and FEM and FVM modeling.